



HAL
open science

Exosomal miRNA profiling from H5N1 avian influenza virus-infected chickens

Yejin Hong, Anh Duc Truong, Jiae Lee, Thi Hao Vu, Sooyeon Lee, Ki-Duk Song, Hyun S. Lillehoj, Yeong Ho Hong

► **To cite this version:**

Yejin Hong, Anh Duc Truong, Jiae Lee, Thi Hao Vu, Sooyeon Lee, et al.. Exosomal miRNA profiling from H5N1 avian influenza virus-infected chickens. *Veterinary Research*, 2021, 52 (1), pp.36. 10.1186/s13567-021-00892-3 . hal-03161701

HAL Id: hal-03161701

<https://hal.science/hal-03161701v1>

Submitted on 8 Mar 2021

HAL is a multi-disciplinary open access archive for the deposit and dissemination of scientific research documents, whether they are published or not. The documents may come from teaching and research institutions in France or abroad, or from public or private research centers.


L'archive ouverte pluridisciplinaire **HAL**, est destinée au dépôt et à la diffusion de documents scientifiques de niveau recherche, publiés ou non, émanant des établissements d'enseignement et de recherche français ou étrangers, des laboratoires publics ou privés.

RESEARCH ARTICLE

Open Access



Exosomal miRNA profiling from H5N1 avian influenza virus-infected chickens

Yejin Hong¹, Anh Duc Truong², Jiae Lee¹, Thi Hao Vu¹, Sooyeon Lee¹, Ki-Duk Song³, Hyun S. Lillehoj⁴ and Yeong Ho Hong^{1*} 

Abstract

Exosomes are membrane vesicles containing proteins, lipids, DNA, mRNA, and micro RNA (miRNA). Exosomal miRNA from donor cells can regulate the gene expression of recipient cells. Here, Ri chickens were divided into resistant (*Mx/A; BF2/B21*) and susceptible (*Mx/G; BF2/B13*) trait by genotyping of *Mx* and *BF2* genes. Then, Ri chickens were infected with H5N1, a highly pathogenic avian influenza virus (HPAIV). Exosomes were purified from blood serum of resistant chickens for small RNA sequencing. Sequencing data were analysed using FastQCv0.11.7, Cutadapt 1.16, miRBase v21, non-coding RNA database, RNAcentral 10.0, and miRDeep2. Differentially expressed miRNAs were determined using statistical methods, including fold-change, exactTest using edgeR, and hierarchical clustering. Target genes were predicted using miRDB. Gene ontology analysis was performed using gProfiler. Twenty miRNAs showed significantly different expression patterns between resistant control and infected chickens. Nine miRNAs were up-regulated and 11 miRNAs were down-regulated in the infected chickens compared with that in the control chickens. In target gene analysis, various immune-related genes, such as cytokines, chemokines, and signalling molecules, were detected. In particular, mitogen-activated protein kinase (MAPK) pathway molecules were highly controlled by differentially expressed miRNAs. The result of qRT-PCR for miRNAs was identical with sequencing data and miRNA expression level was higher in resistant than susceptible chickens. This study will help to better understand the host immune response, particularly exosomal miRNA expression against HPAIV H5N1 and could help to determine biomarkers for disease resistance.

Keywords: H5N1, HPAIV, Exosomes, Small RNA sequencing, miRNA

Introduction

Exosomes are membrane vesicles, approximately 40–100 nm in diameter, and present in most biological fluids [1–3]. Exosomes are derived from multivesicular bodies (MVBs) to form intraluminal vesicles (ILVs), which are then released into the extracellular environment as exosomes after fusion with the plasma membrane [3]. Lipids and proteins are the main components of exosomes and various nucleic acids, such as mRNAs,

microRNAs (miRNAs), and other non-coding RNAs (ncRNAs), and are also found in the exosomal lumen [1–4]. These exosomal RNAs can be delivered from donor cells to recipient cells, wherein they modulate various biological systems [5–7]. Therefore, exosomes are important in cell-to-cell communication.

miRNAs are small ncRNA molecules and are typically 22 nucleotides in length, which repress translation of the target mRNA by binding to the 3'-untranslated region and/or induce the decay of up to 30% of all expressed transcripts [8]. miRNAs are involved in diverse biological processes, including fat metabolism; cell death, proliferation, differentiation; and the functioning of the immune

*Correspondence: yhong@cau.ac.kr

¹ Department of Animal Science and Technology, Chung-Ang University, Anseong 17546, Republic of Korea

Full list of author information is available at the end of the article



© The Author(s) 2021. This article is licensed under a Creative Commons Attribution 4.0 International License, which permits use, sharing, adaptation, distribution and reproduction in any medium or format, as long as you give appropriate credit to the original author(s) and the source, provide a link to the Creative Commons licence, and indicate if changes were made. The images or other third party material in this article are included in the article's Creative Commons licence, unless indicated otherwise in a credit line to the material. If material is not included in the article's Creative Commons licence and your intended use is not permitted by statutory regulation or exceeds the permitted use, you will need to obtain permission directly from the copyright holder. To view a copy of this licence, visit <http://creativecommons.org/licenses/by/4.0/>. The Creative Commons Public Domain Dedication waiver (<http://creativecommons.org/publicdomain/zero/1.0/>) applies to the data made available in this article, unless otherwise stated in a credit line to the data.

system [9]. Therefore, exosomal miRNAs from donor cells can regulate the gene expression of recipient cells. Furthermore, the composition of exosomal miRNAs is different between healthy and diseased individuals [10]. Thus, exosomal miRNAs indicate the state of disease and control the immune systems.

Avian influenza viruses (AIV) in *Influenzavirus A* genus, belonging to the family *Orthomyxoviridae*, cause severe outbreaks in the poultry industry. In particular, the H5N1 subtype is a highly pathogenic avian influenza virus (HPAIV) that originated from Asia [11]. H5N1 in poultry decreases egg production and causes rhinorrhoea, loss of appetite, soft-shelled or misshapen eggs, diarrhoea, and sudden death [12]. Thus, H5N1 outbreak causes significant economic damage to the poultry industry. Furthermore, H5N1 can be transmitted to humans and causes severe acute respiratory infection with a fatality rate of more than 50% [13]. Therefore, it is essential to elucidate the mechanisms of AIV pathogenesis in chickens to control the infection.

Exosomes have various roles in immune response by delivering exosomal contents to other cells such as membrane-bound receptors and miRNAs [14]. Therefore, we suggest that exosomes might have important roles, especially delivering miRNAs, in immune response against infection of H5N1 HPAIV. To date, however, there are no studies describing exosomal small RNA transcriptome analysis in AIV infection. In this study, Ri chickens, local yellow-feathered household chickens of Vietnam [15], were used as experimental animals. Further, by genotyping the *Mx* and *BF2* gene, Ri chickens resistant and susceptible to AIV were distinguished. The *Mx* protein, which is part of the dynamin family of large GTPases, interferes with the replication of RNA viruses by inhibiting trafficking or the activity of viral polymerases [16–18]. The chicken major histocompatibility complex (MHC) consists of *BLB* (Class II) and two *BF* (Class I) [19, 20]. Especially, among haplotype of *BF2*, *B21* allele is associated with high antibody titer against infectious bursal disease virus [21, 22]. Moreover, the chickens with *B21* haplotype have high survival rate and with *B13* have high mortality rate against H5N1 AIV [23]. To identify the profiling of exosomal miRNA against AIV infection, we infected Ri chickens with the AIV subtype H5N1 and purified exosomes from the serum for small RNA sequencing and analysis.

Materials and methods

Experimental birds and genotyping

All specific-pathogen-free (SPF) Ri chickens [15], a native Vietnamese chicken breed, were infected with AIV and observed daily for signs of disease and mortality. All chicken experiments were performed in our collaborative

laboratory at the Department of Biochemistry and Immunology in the National Institute of Veterinary Research, Vietnam. A total of 40 Ri chickens belonging to resistant and susceptible lines were used in our study (see Additional file 1).

Genotyping of *Mx* and *BF2* was performed by high resolution melt analysis for resistance and susceptibility selection [16–18, 22, 23]. In detail, the polymorphism of allele A/G of *Mx* at position 631 demonstrated allele A (resistant trait) and allele G (susceptible trait) in Ri chickens (see Additional file 2). Among *BF2* haplotype, Ri chickens that have *B21* haplotype were selected as a resistant trait and *B13* haplotype were selected as a susceptible trait. Finally, Ri chickens *Mx(A)/B21* were selected as a resistant trait and *Mx(G)/B13* were selected as a susceptible trait. For HPAIV challenge, a total of 20 4-week-old birds, 10 Ri chickens in each line, received intranasal inoculation of 200 μ L of harvested allantois fluid of the infected eggs, containing 1×10^4 50% egg infectious dose (EID₅₀) [24] of A/duck/Vietnam/QB1207/2012 (H5N1), according to the OIE guideline.

Exosome extraction and characterization

Blood samples were collected from the wing vein of chickens after 1 and 3 days of infection (three chickens from each group). Exosomes were extracted from the serum using Total Exosome Isolation Reagent (Invitrogen, Carlsbad, CA, USA), according to the manufacturer's protocol. Briefly, 5 mL of the blood sample was collected from infected and control chickens. The blood was incubated at room temperature (RT) for 2 h to allow clotting. Serum was isolated from the clotted blood and centrifuged at $2000 \times g$ for 30 min at 4 °C to remove cells and debris. The supernatant was mixed with 0.2 volumes of the Total Exosome Isolation reagent and incubated at 4 °C for 30 min. After incubation, samples were centrifuged at $10\,000 \times g$ for 10 min at RT. The supernatant was discarded, and exosomes were contained in the pellet at the bottom of the tube. Exosomes were suspended with phosphate-buffered saline (PBS; pH 7.4) and stored at ≤ -20 °C.

For characterization of exosomes, the particle size was measured using a Nanoparticle Analyzer (HORIBA, SZ-100, Kyoto, Japan). Furthermore, a Western blot assay was performed using CD81 as an exosomal marker (#56039; Cell Signaling Technology, Danvers, MA, USA) according to previously described methods [25].

Exosomal RNA extraction and small RNA sequencing

Small RNA sequencing was conducted using exosomes from resistant Ri chickens at day 3 post-infection. Exosomal RNA was extracted using the miRNeasy Serum/Plasma Kit (Qiagen, Hilden, Germany) according to the

manufacturer's protocol. Library construction and small RNA sequencing were only conducted for resistant Ri chickens with 1 control (Resistant day-3) and 2 infection (Resistant day-3) samples. The library was constructed using SMARTer smRNA-Seq Kit for Illumina (TAKARA Bio Inc., Otsu, Shiga, Japan) according to the manufacturer's protocol. Next, small RNA sequencing was conducted by Macrogen (Seoul, Republic of Korea) using a HiSeq 2500 System (Illumina Inc., San Diego, CA, USA).

Bioinformatic analysis of sequencing data

The raw sequence reads were filtered based on quality using FastQC v0.11.7 [26]. Adapter sequences were trimmed off the raw sequence reads using Cutadapt 1.16 [27]. Both the trimmed and non-adapter reads were used as processed reads to analyze long targets (≥ 50 bp). Unique clustered reads were sequentially aligned to the reference genome using miRBase v21 [28], and the non-coding RNA database, RNACentral 10.0 [29], to classify known miRNAs and other RNA types, such as tRNA, small nuclear RNA (snRNA), and small nucleolar RNA (snoRNA). Novel miRNA prediction was performed by miRDeep2 [30]. The read counts for each miRNA were extracted from mapped miRNAs to report the abundance of each miRNA. Differentially expressed miRNAs were determined by comparing each miRNA across conditions using statistical methods, such as fold-change, exactTest using edgeR (Empirical Analysis of Digital Gene Expression Data in R), and hierarchical clustering. Target genes of differentially expressed miRNAs were predicted using miRDB [31] and target genes with a target score over 80 were selected. Next, GO functional enrichment analysis of target genes was performed using gProfiler [32]. The miRNA-mRNA network were constructed using miRNet [33].

miRNA primer design

Quantitative real-time PCR (qRT-PCR) for miRNAs only required a forward primer to be designed for the individual miRNA. The reverse primer was a universal primer provided with the miScript SYBR Green PCR Kit (Qiagen). All known chicken miRNA sequences were obtained from miRBase [34]. Oligonucleotide primers for these miRNAs were designed using full-length mature miRNA sequences. Primers were synthesized by Genotech (Daejeon, South Korea) (see Additional file 3).

miRNA expression analysis by qRT-PCR

For qRT-PCR, susceptible control (3 samples of day-3), susceptible infection (2 samples of day-3), resistant control (1 sample of day-3), and resistant infection (2 samples of day-3) RNA samples were used. cDNA

synthesis was performed using miScript II RT Kit (Qiagen) according to the manufacturer's protocol. Briefly, 1 μ g of total RNA was combined with 4 μ L of 5 \times miScript HiSpec Buffer, 2 μ L of 10 \times miScript Nucleics Mix, 2 μ L of miScript Reverse Transcriptase Mix, and RNase-free water up to 20 μ L. The tube was incubated at 37 $^{\circ}$ C for 60 min and at 95 $^{\circ}$ C for 5 min to inactivate miScript Reverse Transcriptase Mix and kept on ice. Next, 20 μ L of reverse-transcription reaction mixtures were diluted with 130 μ L of RNase-free water. The synthesized cDNA was used as a template for qRT-PCR. miScript SYBR Green PCR Kit (Qiagen) was used to determine miRNA expression in LightCycler 96 system (Roche, Indianapolis, IN, USA) according to the manufacturers' protocol. In brief, for 25 μ L of reaction mix, the following components were added: 12.5 μ L of 2 \times QuantiTect SYBR Green PCR Master Mix, 2.5 μ L of 10 μ M forward primer, 2.5 μ L of 10 \times universal primer, 2.5 μ L of template cDNA, and RNase-free water up to 25 μ L. The cycling conditions were as follows: 95 $^{\circ}$ C for 15 min to activate as the initial step, followed by 45 cycles of 94 $^{\circ}$ C for 15 s, 55 $^{\circ}$ C for 30 s, and 70 $^{\circ}$ C for 30 s. Gene expression was calculated using the $2^{-\Delta\Delta Ct}$ method after normalization with U1A (5'-CTGCATAATTGTGGTAGTGG-3') [35]. All qRT-PCRs were performed in triplicate.

Statistical analysis

Statistical analysis was performed using SPSS 25.0 software (IBM, Chicago, IL, USA). Data are expressed as mean values \pm SEM. Statistical comparisons were performed using Student's *t*-test for two-group comparisons, and the level of statistically significant difference was set at $p < 0.05$.

Results

Exosomal small RNA analysis

Exosomes were purified from the serum of resistant and susceptible Ri chickens at day 3 post-infection. The size and markers of exosomes were identified (see Additional file 4). Small RNA sequencing was conducted on resistant Ri chickens. In the control sample (Non-infected Ri chickens), 61 116 319 reads were produced, and total read bases were 3.1 Gbp (Table 1). In HPAIV-infected samples, 54 035 519 reads and 2.8 Gbp of read bases were produced. The GC content of control was 38.63% and the ratio of bases with Phred quality score ≥ 30 (Q30) was 90.99%. The GC content of infected chickens was 40.10% and the Q30 was 92.53%. Additional file 5 shows the read length distribution of each sample. In the control, a read length of approximately 17–20 bp was more abundant, whereas the read length was evenly distributed in infected chickens. For

Table 1 Raw data statistics

Sample	Total reads bases	Total reads	Processed reads	Mapped reads	GC (%)	Q20 (%)	Q30 (%)	Known miRNA in sample	Known miRNA in chicken (miRBase v21)
Control	3 116 932 269	61 116 319	46 317 909	26 209 (0.06%)	39	95	91	152	994
Infection	2 755 811 469	54 035 519	47 254 454	16 389 (0.03%)	40	96	93	136	994

Total reads bases = total read × read length. Total read bases indicate the total number of bases sequenced and total reads indicate the total number of reads. Processed reads indicate reads that were trimmed and unwanted sources were deleted. Q20 (%) is the ratio of bases with Phred quality score of ≥ 20. Q30 (%) is the ratio of bases with Phred quality score of ≥ 30.

control and infected samples, final processed reads were sequentially aligned to the reference genome and the miRBase v21 and ncRNA databases to classify the known miRNAs and other types of RNA, such as tRNA, snoRNA, snRNA, and Piwi-interacting RNA (piRNA) (see Additional file 6). In the control, genome sequences are the largest part as a 92.56% and known miRNA, novel miRNA, snoRNA, snRNA, rRNA, tRNA account for 0.05%, 1.21%, 0.15%, 18.42%, 5.44%, and 0.03%, respectively. Also, genome sequences of the infected samples comprised the largest part (94.1%) and known miRNA, novel miRNA, snoRNA, snRNA, rRNA, and tRNA accounted for 0.03%, 0.32%, 0.04%, 6.46%, 2.25%, and 0.02%, respectively. To predict the known and novel miRNA, unique clustered reads were aligned against the reference genome and precursor miRNAs separately. Novel miRNAs are predicted from mature, star and loop sequence according to the RNA-fold algorithm using miRDeep2. To detect known and

novel miRNAs, miRDeep2 estimated their abundance (Table 1). In the control, among total 46 317 909 reads, 84.78% (39 269 083 reads) were mapped and 15.22% (7 048 826 reads) were unmapped reads. In infected chickens, among 47 254 454 reads, 90.21% (42 628 445 reads) were mapped and 9.79% (4 626 009 reads) were unmapped reads. We also investigated differentially expressed miRNA analysis by the read count value of mature miRNAs (see Additional file 7). A total of 20 miRNAs showed significantly different fold-change (Figure 1). Among 20 miRNAs, nine miRNAs were up-regulated and 11 miRNAs were down-regulated in infected chickens compared to those in the control. In particular, gga-miR-222a was the highest, with a fold-change of 8.69, and gga-miR-1434 was the lowest, with fold-change of -8.36. gga-miR-222a, gga-miR-30c-1-3p, gga-miR-126-5p, gga-miR-24-3p, gga-miR-101-3p, gga-miR-142-5p, gga-miR-2954, gga-miR-214, and gga-let-7g-5p were up-regulated in infected

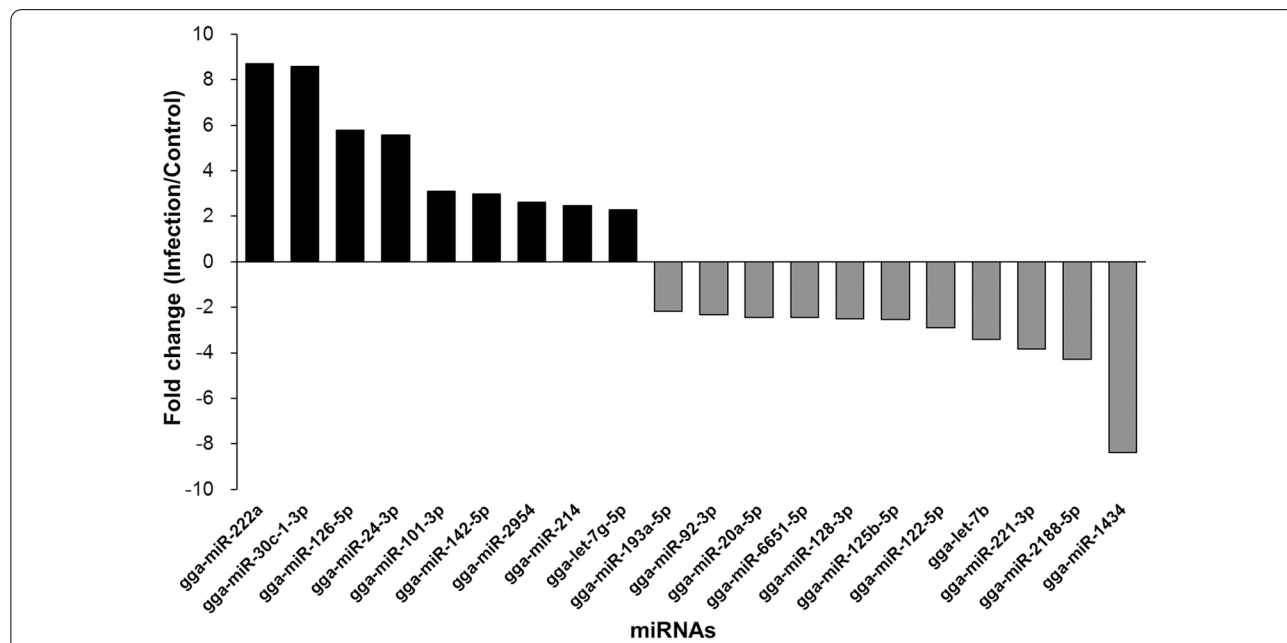


Figure 1 Differentially expressed miRNA analysis. Fold-change of 20 miRNAs in the control and avian influenza virus-infected samples. Statistical analysis was performed using fold-change, and significant results were selected on conditions of $|FC| \geq 2$ and exactTest raw p -value < 0.05 .

samples compared with that in the control, whereas gga-miR-193a-5p, gga-miR-92-3p, gga-miR-20a-5p, gga-miR-6651-5p, gga-miR-128-3p, gga-miR-125-5p, gga-miR-122-5p, gga-let-7b, gga-miR-221-3p, gga-miR-2188-5p, and gga-miR-1434 were down-regulated in infected samples compared with those in the control. We also compared the expression levels of miRNAs between control and infected samples using a volcano plot (Figure 2). Log₂ fold-change and *p*-values obtained from the comparison between the two groups were plotted as a volcano plot. gga-miR-1434 displayed both high fold-change (x-axis) and statistical significance (y-axis). We also conducted hierarchical clustering analysis by the Euclidean method and complete linkage, which clusters similar mature miRNAs and samples by expression level (normalized value) from the differentially expressed miRNA list (Figure 3). Nine up-regulated exosomal miRNAs in the infected chickens were grouped in the generated dendrogram.

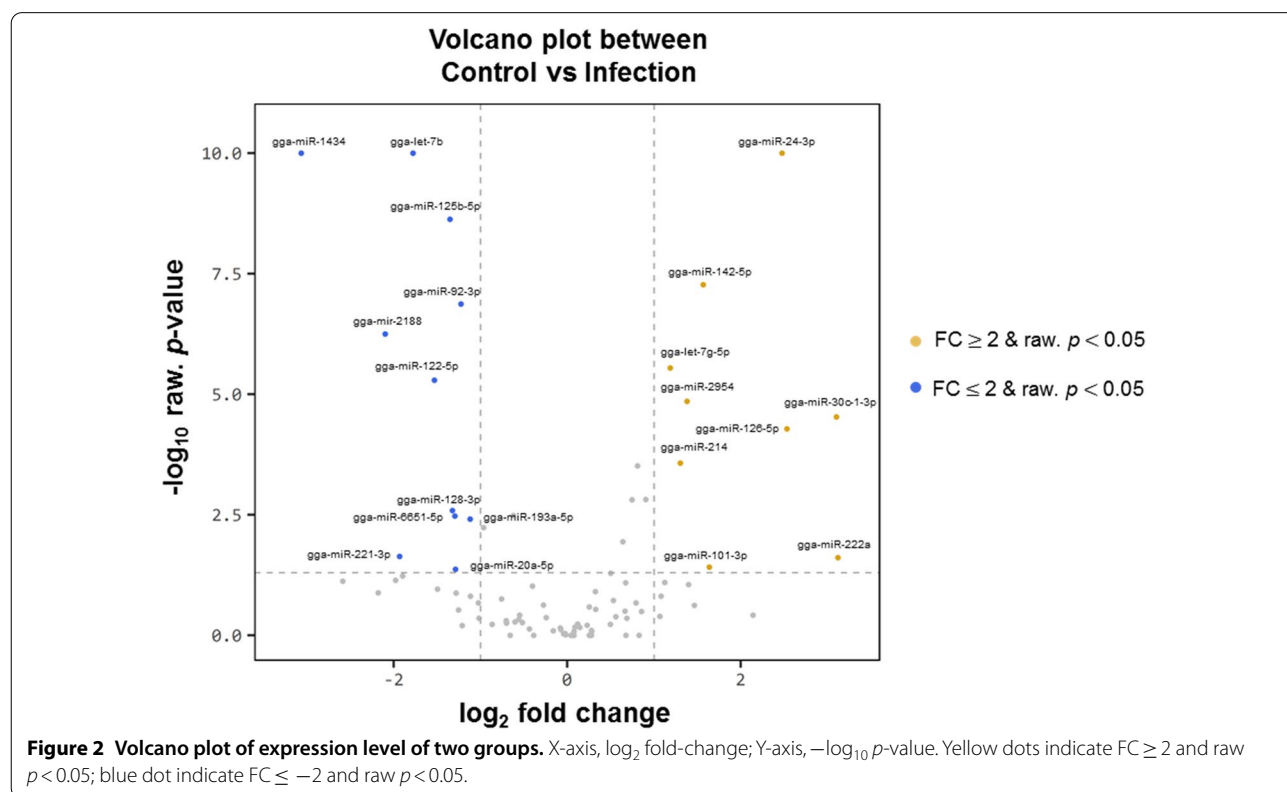
Target gene prediction, GO functional enrichment, and Kyoto Encyclopedia of Genes and Genomes (KEGG) pathway analysis

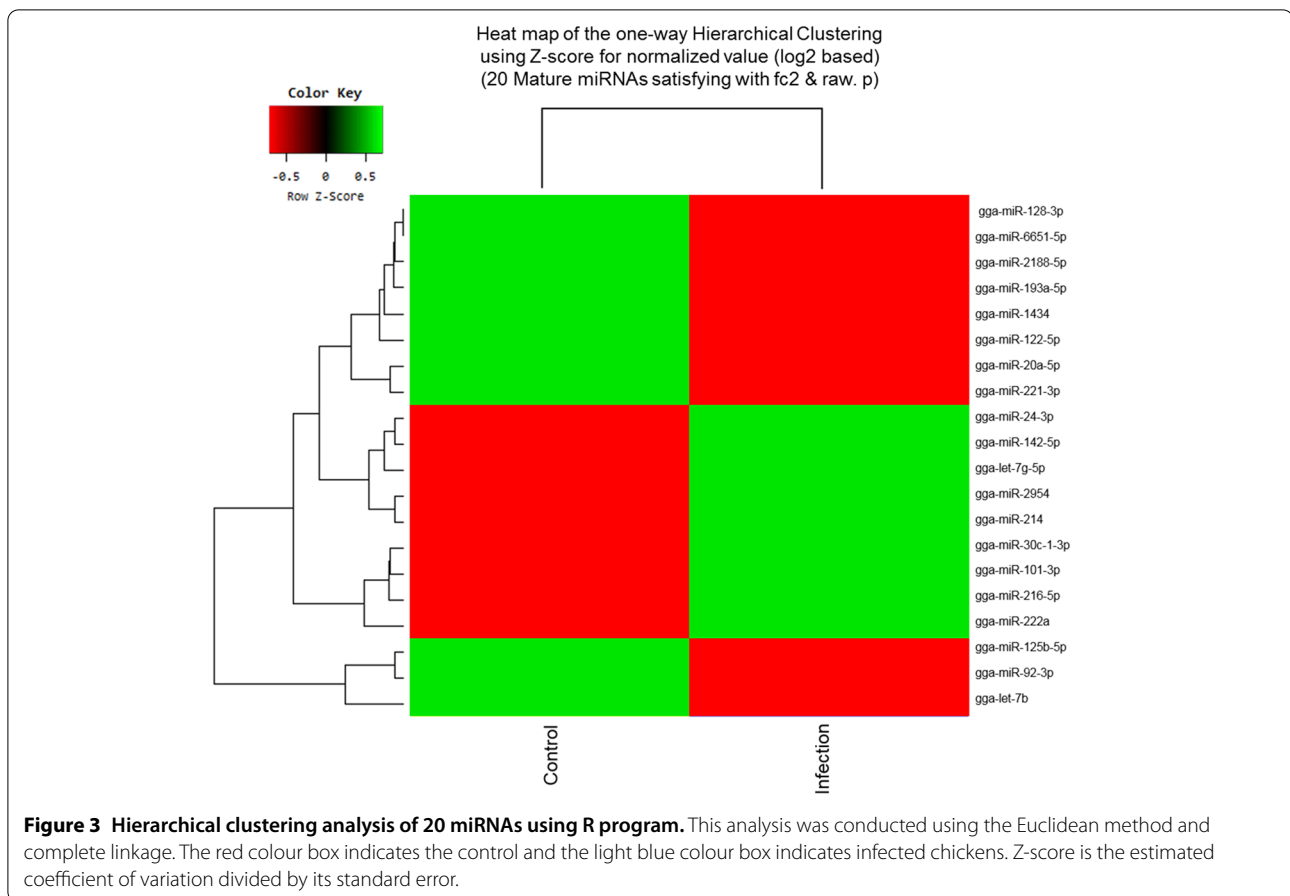
The target genes of 20 miRNAs were predicted using miRDB. Immune-related target genes with score of over 80 were selected (Table 2). In particular, 32

immune-related genes were related to gga-miR-20a-5p, and no immune-related target genes were related to gga-miR-1434. We also conducted GO analysis using gProfiler (see Additional file 8). In KEGG pathway analysis, eight pathways, including erythroblastic leukemia viral oncogene homolog (ErbB) signalling pathway, advanced glycation end-products (AGE)–receptor of AGE (RAGE) signalling pathway in diabetic complications, mitogen-activated protein kinase (MAPK) signalling pathway, focal adhesion, regulation of actin cytoskeleton, insulin signalling pathway, phosphatidylinositol signalling system, and endocytosis, were related to 20 miRNAs (Table 3). In particular, 69 target genes of miRNAs were related with the MAPK signalling pathway, followed by endocytosis (59 genes), focal adhesion (52 genes), and regulation of actin cytoskeleton (52 genes). Furthermore, the miRNA-mRNA target gene interaction of 20 differentially expressed miRNAs was analysed. As shown in Figure 4, several targets genes were shared with more than two miRNAs.

Validation of miRNA expression by qRT-PCR

qRT-PCR was conducted using four miRNAs, selected on the basis of significant difference of >2.0 or <2.0 fold-change between control and infected chickens, to validate sequencing results (Figure 5A). The four miRNAs were





selected based on read count, the number of immune-related genes, and functions in immune system. The expression levels of gga-miR-30c-1-3p, gga-miR-214, and gga-let-7g-5p were up-regulated in infected resistant chickens compared with those in the control by 2.85, 3.37, and 23.91 fold-change, respectively. However, the expression of gga-let-7b was down-regulated in infected chickens (0.34 fold-change). qRT-PCR results of the four miRNAs were positively correlated with sequencing results. The expression levels of gga-miR-214 and gga-let-7b were also evaluated in resistant and susceptible Ri chickens (Figure 5B). The expression level of gga-miR-214 was up-regulated in susceptible infected chickens compared with that in the control (3.48 fold-change). However, the expression level of gga-let-7b was down-regulated in susceptible infected chickens compared with that in the control (0.57 fold-change). The expression patterns of gga-miR-214 and gga-let-7b were similar in susceptible and resistant chickens. Moreover, the expression levels of gga-miR-214 and gga-let-7b were higher (2.79 and 17.18 fold-change, respectively) in resistant chickens than in susceptible chickens. Furthermore, the expression of four miRNAs was compared between susceptible and

resistant mock control (Figure 5C). The expression levels of gga-miR-214, gga-miR-30c-1-3p, gga-let-7g-5p, and gga-let-7b were higher in resistant than susceptible control chicken (2.88, 45.67, 180.39, and 28.34 fold-change, respectively).

Discussion

In this study, we report exosomal miRNA analysis of avian influenza virus infected chickens. The Vietnamese AIV-resistant Ri chickens were selected by *Mx* and *BF2* genotyping and infected with H5N1 HPAIV. Then, exosomes were isolated from the serum, and miRNA was analysed by small RNA sequencing and qRT-PCR.

Exosomes are formed by various molecules, such as proteins, lipids, DNA, mRNA, and miRNA, that are contained in endosomes through endocytosis. Then, endosomes called MVBs fuse with the cell membrane and are released into the extracellular space [36]. Released exosomes containing miRNA are delivered to other cells through biological fluids and regulate the gene expression of recipient cells; however, they are not randomly packaged in exosomes [37–40].

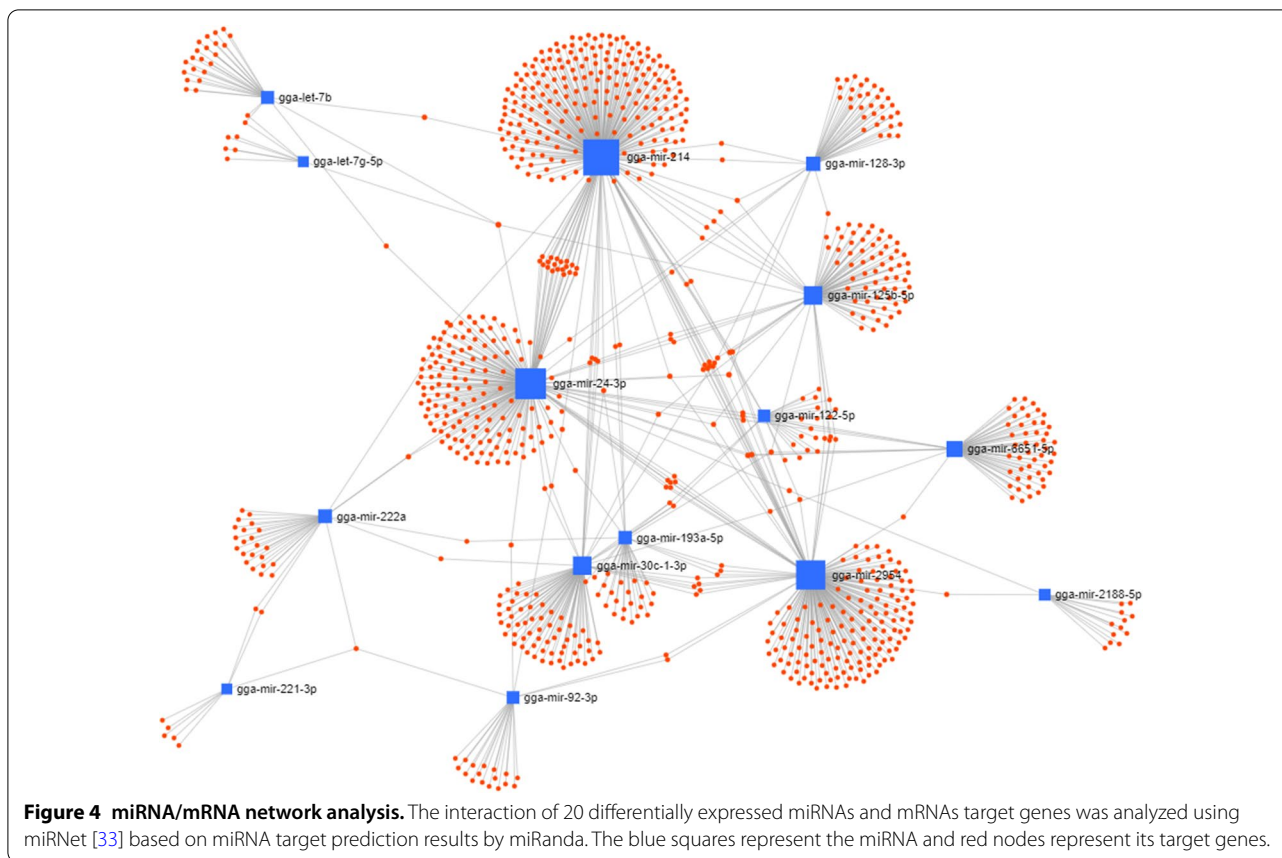
Table 2 Immune-related target genes for miRNAs

miRNAs	Fold change (infection/control)	Immune related target genes	Gene symbol	Control read count	Infection read count
gga-let-7b	-3.425194	24	IGDCC3, COL4A1, COL4A2, AGO4, LRIG3, COL1A2, IL13RA1, LRIG1, MAPK6, TGFB1, IGDCC4, COL3A1, TNFAIP2, WNT9B, SEC14L1, DCLRE1C, ERCC6, CCR6, MAP4K3, EDN1, TBKBP1, MAP3K1, MAP4K4, FGF6	8110	1943
gga-let-7 g-5p	2.2773292	14	IL13RA1, MAPK6, TGFB1, WNT9B, SEC14L1, DCLRE1C, CCR6, ERCC6, MAP4K3, MAP3K1, EDN1, TBKBP1, MAP4K4, FGF6	146	273
gga-miR-101-3p	3.110288	21	MAP3K13, MAPK6, CD274, MAP3K9, CREB1, MAP3K4, BACH2, MAPK1, NLK, CCR2, PIK3CG, SYNCRIP, SH3GL3, MEF2A, MAPK8, HACD3, MAPKAPK5, NF1, STAT3, CAMK2D, TRAF3	5	13
gga-miR-122-5p	-2.889137	1	GREM2	127	36
gga-miR-125b-5p	-2.550591	8	IRF4, PTPN1, SMURF1, PRDM1, TSTA3, IL17RA, TRAF3IP2, IL13RA1	1001	322
gga-miR-126-5p	5.7802815	17	LIF, TRAF3, FGFRL1, FGF12, C6, C1S, FGF7, IL17A, DENND1B, FGF14, CREB1, MAPK10, GATA3, SARM1, ERAP1, GDF9, JAG1	6	29
gga-miR-128-3p	-2.500261	26	JAG1, GAB1, MAPK8IP3, NF1, ZFP36L1, DAB2IP, SH3BGRL2, NCF1, MAPK14, MAPKBP1, C1S, IL9R, WNT2, MAP2K3, ITCH, DENND1B, TSC1, SH3RF1, SETX, FGF14, TRIL, IL17RA, PTPRC, RAB20, JAK2, PRDM11	52	17
gga-miR-142-5p	2.9630095	7	IL8L1, ITCH, TAB3, SFPQ, MAP4K4, FGF10, BMP15	69	168
gga-miR-1434	-8.369591	0		103	10
gga-miR-193a-5p	-2.172781	1	PDCD1LG2	69	26
gga-miR-20a-5p	-2.441626	32	MAP3K2, IL1RAPL1, CD274, PDCD1LG2, TGFB2, BPIFB3, SOS1, ITCH, GAB1, MAP3K14, IPO7, MAPK1, MAP3K9, PRDM11, TNFRSF21, FAM3C, CREB5, GPI, TGFBRAP1, SMAD6, AKT3, TOLLIP, SH3PXD2A, SH3GLB2, MAP3K5, PKD1, CAMK2D, MAP1LC3A, TNFSF11, CREB1, SAMHD1, IL17RD	24	8
gga-miR-214	2.464608	16	SOS2, IRF8, MAPK1, EPHB6, TAB3, FGF14, LIF, DMAP1, DNAJA3, CD8A, NF1, PIK3CG, SH3PXD2A, TRAF3, LACC1, CCR2	37	75
gga-miR-2188-5p	-4.285245	4	FOSB, FGF20, PAK3, JUN	84	16
gga-miR-221-3p	-3.818655	8	PRDM1, ANKHD1, FOS, TAB2, CSF1R, ERBB4, IPO7, SMURF2	19	4
gga-miR-222a	8.6921924	8	PRDM1, ANKHD1, FOS, CSF1R, TAB2, ERBB4, IPO7, SMURF2	1	8
gga-miR-24-3p	5.5548592	2	MAPKAP1, OTUD7B	51	233
gga-miR-2954	2.6033041	4	TJP2, SYK, NFIL3, CD274	50	107
gga-miR-30c-1-3p	8.5887224	7	SCG2, LIFR, TAB3, TRAF2, MAP3K3, TOLLIP, SEC14L1	3	22
gga-miR-6651-5p	-2.452306	4	HIF1A, ELMOD2, LTA4H, AvBD8	51	17
gga-miR-92-3p	-2.335071	15	SMURF1, MAP2K4, DENND1B, RORA, MAP3K20, G3BP2, SH3PXD2A, TSC1, PIK3CD, GREM2, GSN, LRRK2, DNAJB9, TRAF3, UBASH3B	703	247

Table 3 KEGG pathway analysis

KEGG	Pathway	Gene Count	p-value
KEGG:04012	ErbB signalling pathway	29	5.87E-04
KEGG:04933	AGE-RAGE signalling pathway in diabetic complications	31	8.56E-04
KEGG:04010	MAPK signalling pathway	69	1.05E-03
KEGG:04510	Focal adhesion	52	1.15E-03
KEGG:04810	Regulation of actin cytoskeleton	52	6.02E-03
KEGG:04910	Insulin signalling pathway	36	7.88E-03
KEGG:04070	Phosphatidylinositol signalling system	30	1.02E-02
KEGG:04144	Endocytosis	59	1.36E-02

In this study, 20 exosomal miRNAs exhibited significantly different expression between control and infected resistant Ri chickens (Figure 1). Previous studies have reported differentially expressed miRNA in chickens and humans. The expression of gga-miR-6651-5p increases in Marek's disease virus infected-chickens [41]; gga-miR-92-3p and gga-miR-214 are abundant in AIV H9N2-infected chicken embryo fibroblasts [42]; gga-miR-2954 is up-regulated in reticuloendotheliosis virus-infected chickens [43]; gga-miR-222a, gga-miR-125b-5p, and gga-miR-128-3p are down-regulated in H9N2-infected chicken embryo fibroblasts [42]. Likewise, in our study, gga-miR-125b and gga-miR-128-3p were down-regulated in H5N1-infected chickens. In another study, miR-126-5p

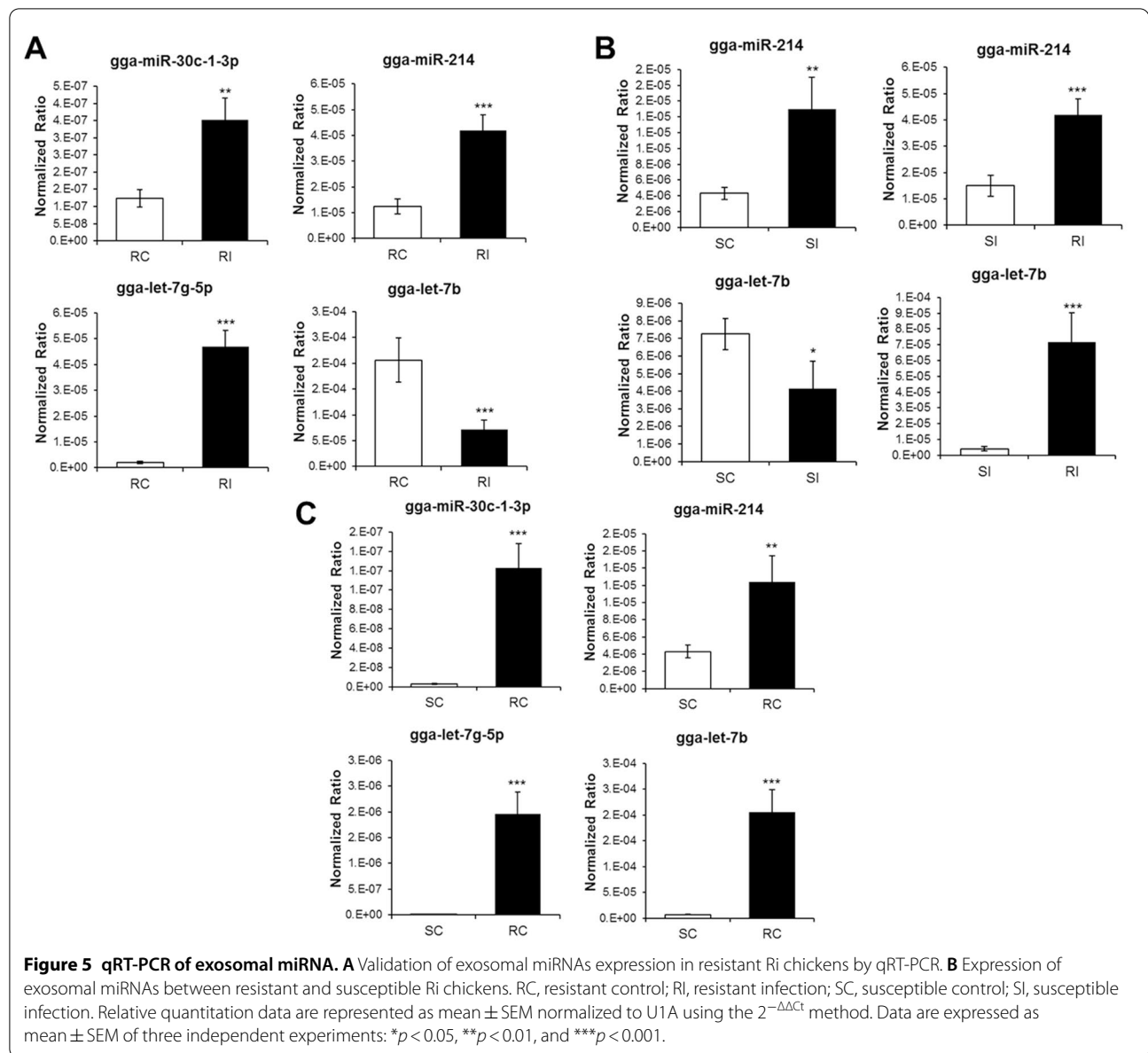


inhibited human cervical cancer progression, thus, regulating the apoptosis of cancer cells [44]. gga-miR-101-3p is up-regulated in *Mycoplasma gallisepticum*-infected chickens [45]. gga-let-7b and miR-128 reduce cell growth and division during skeletal muscle development in sex-linked dwarf chickens [46]. gga-let-7b is involved in signalling pathways, such as MAPK, TGF- β , Notch, Wnt, mTOR, cell cycle, p53, and Janus-activated kinase (JAK)-signal transducers and activators of transcription (STAT) pathways [47]. Human miR-20a-5p inhibits cell proliferation and induces apoptosis in SH-SY5Y cells [48], and its down-regulation induces cell apoptosis to remove mycobacterial cells through targeting JNK2 in human macrophages [49]. Therefore, we suggest that 19 differentially expressed exosomal miRNAs from AI-infected chickens regulate immune response.

We analysed immune-related target genes (Table 2). Various immune-related genes, such as genes encoding signalling pathway molecules, cytokines, and chemokines, were found to be miRNA target genes. In particular, in KEGG pathway analysis, the highest number of target genes (69 gene count) were related with the MAPK signalling pathway (Table 3). The MAPK signalling pathway plays important roles in the immune system

and also in cell proliferation, differentiation, migration, and apoptosis [50]. MAPK signalling pathway was activated by H5N1 AIV [51–53]. Several molecules of the MAPK pathway are differently regulated in two inbred necrotic enteritis-afflicted chicken lines, 6.3 and 7.2 [54]. Furthermore, the MAPK pathway plays an important role in virus replication in chicken macrophages infected with H9N2 AIV [55]. MAPK signalling pathway was followed by Endocytosis (59 gene count). As a first step of AIV infection, AIV enters the cells by endocytosis [56]. The next KEGG pathway was Focal adhesion and regulation of actin cytoskeleton (52 gene count). Focal adhesion kinase was activated during AIV infection by inducing actin rearrangement [57]. Therefore, we suggest that the target genes of 20 exosomal miRNAs regulate pro-inflammatory signalling pathway against AIV infection and life cycle of AIV.

We also compared the expression of gga-miR-214 and gga-let-7b between resistant and susceptible Ri chickens (Figure 4B). The expression patterns between control and infected chickens were the same, but the expression levels were higher in resistant than in susceptible chickens. Therefore, we suggest that the copy number of miRNAs is higher in the exosomes of resistant Ri chickens than



in the exosomes of susceptible Ri chickens. Accordingly, regulation of gene expression by exosomal miRNAs may be higher in resistant Ri chickens. Hence, resistant Ri chickens could respond more actively than susceptible Ri chickens against AIV infection.

So far, several studies have analysed miRNA expression patterns on AIV infection [45, 58–61]. However, there have limited studies on the exosomes in chickens until now.

Taken together, this study provides an insight into the exosomal miRNA expression pattern in AIV-resistant

and -susceptible chickens and the mechanism by which they regulate target genes toward HPAIV infection.

In summary, we have, for the first time, analysed the exosomal miRNA expression in H5N1 HPAIV-infected chickens by small RNA sequencing and qRT-PCR. A total of 20 miRNAs were differentially expressed in exosomes of control and infected resistant Ri chickens. Interestingly, most of the target genes were related with the MAPK signalling pathway. This study improves our understanding of the host immune response, particularly

with respect to exosomal miRNA expression, against H5N1 HPAIV infection.

Supplementary Information

The online version contains supplementary material available at <https://doi.org/10.1186/s13567-021-00892-3>.

Additional file 1. Number of Ri chicken samples in each group

Additional file 2. Sequencing analysis of Mx in avian influenza virus-resistant and -susceptible Ri chickens

Additional file 3. Sequences of primers for qRT-PCR analysis

Additional file 4. Characterization of purified exosomes. (A) Particle size distribution measured by Nanoparticle Analyzer. (B) Western blotting of exosomes with exosomal marker CD81.

Additional file 5. Read length distribution of control and infection samples. Generally mature miRNAs are 20 ~ 25 nt in length.

Additional file 6. Bar plot of RNA composition in the control and avian influenza virus-infected samples. Final processed reads were aligned to small RNAs (≤ 50 ; piRNA) of the database using bowtie [62] and other small RNAs (≥ 50 nt; tRNA, snoRNA, etc.) of the database using bowtie2, which assigned a result of $\geq 90\%$ coverage to the corresponding RNA.

Additional file 7. Raw small RNA sequencing data.

Additional file 8. Gene ontology analysis. (A) Biological process (B) Cellular component (C) Molecular function. Target categorized in specific functional groups according to gene ontology using Fisher's exact test ($p < 0.01$).

Abbreviations

miRNA: Micro RNA; AIV: Avian influenza viruses; HPAIV: Highly pathogenic avian influenza virus; MAPK: Mitogen-activated protein kinase; MVBs: Multi-vesicular bodies; ILVs: Intraluminal vesicles; ncRNAs: Non-coding RNAs; MHC: Major histocompatibility complex; SPF: Specific-pathogen-free; snRNA: Small nuclear RNA; snoRNA: Small nucleolar RNA; qRT-PCR: Quantitative real-time PCR; KEGG: Kyoto Encyclopedia of Genes and Genomes; ErbB: Erythroblastic leukemia viral oncogene homolog; AGE-RAGE signalling pathway: Advanced glycation end-products-receptor of AGE signalling pathway; JAK-STAT signalling pathways: Janus-activated kinase-signal transducers and activators of transcription pathways.

Acknowledgements

We thank Department of Biochemistry and Immunology in the National Institute of Veterinary Research, Vietnam for performing animal experiments and collecting samples.

Authors' contributions

YH, ADT, KDS, HSL, and YHH designed the experiments. YH, ADT, JL, THV, and SL performed the experiments. YH analyzed the data. YH and YHH wrote the paper. All authors read and approved the final manuscript.

Funding

This research is funded by the Vietnam National Foundation for Science and Technology Development (NAFOSTED) under grant number 106.02-2019.01 (PI: Anh Duc Truong), National Research Foundation grant (NRF-2021R1A2C2C005236) of the Republic of Korea and a NIFA grant (#2017-6701526793) from the USDA.

Availability of data and materials

All data generated or analyzed during this study are included in this published article and its additional information files.

Ethics approval and consent to participate

This study was conducted in compliance with the institutional rules for the care and use of laboratory animals using a protocol approved by the Ministry

of Agriculture and Rural Development, Vietnam (TCVN 8402:2010/TCVN 8400-26:2014).

Competing interests

The authors declare that they have no competing interests.

Author details

¹ Department of Animal Science and Technology, Chung-Ang University, Anseong 17546, Republic of Korea. ² Department of Biochemistry and Immunology, National Institute of Veterinary Research, 86 Truong Chinh, Dong Da, Hanoi 100000, Vietnam. ³ Department of Animal Biotechnology, College of Agricultural and Life Sciences, Jeonbuk National University, Jeonju 54896, Republic of Korea. ⁴ Animal Biosciences and Biotechnology Laboratory, Agricultural Research Services, United States Department of Agriculture, Beltsville, MD 20705, USA.

Received: 21 October 2020 Accepted: 2 January 2021

Published online: 03 March 2021

References

1. Simons M, Raposo G (2009) Exosomes—vesicular carriers for intercellular communication. *Curr Opin Cell Biol* 21:575–581
2. Mathivanan S, Ji H, Simpson RJ (2010) Exosomes: extracellular organelles important in intercellular communication. *J Proteom* 73:1907–1920
3. Gross JC, Chaudhary V, Bartscherer K, Boutros M (2012) Active Wnt proteins are secreted on exosomes. *Nat Cell Biol* 14:1036
4. Sato-Kuwabara Y, Melo SA, Soares FA, Calin GA (2015) The fusion of two worlds: Non-coding RNAs and extracellular vesicles—diagnostic and therapeutic implications. *Int J Oncol* 46:17–27
5. Srikanthan S, Li W, Silverstein RL, McIntyre TM (2014) Exosome poly-ubiquitin inhibits platelet activation, downregulates CD 36 and inhibits pro-atherothrombotic cellular functions. *J Thromb Haemost* 12:1906–1917
6. Tkach M, Théry C (2016) Communication by extracellular vesicles: where we are and where we need to go. *Cell* 164:1226–1232
7. Boulanger CM, Loyer X, Rautou P-E, Amabile N (2017) Extracellular vesicles in coronary artery disease. *Nat Rev Cardiol* 14:259
8. Bartel DP (2004) MicroRNAs: genomics, biogenesis, mechanism, and function. *Cell* 116:281–297
9. He L, Hannon GJ (2004) MicroRNAs: small RNAs with a big role in gene regulation. *Nat Rev Genet* 5:522–531
10. Zhang J, Li S, Li L, Li M, Guo C, Yao J, Mi S (2015) Exosome and exosomal microRNA: trafficking, sorting, and function. *Genom Proteom Bioinf* 13:17–24
11. Xu X, Subbarao K, Cox NJ, Guo Y (1999) Genetic characterization of the pathogenic influenza A/Goose/Guangdong/1/96 (H5N1) virus: similarity of its hemagglutinin gene to those of H5N1 viruses from the 1997 outbreaks in Hong Kong. *Virology* 261:15–19
12. Kullman G (2008) Protecting poultry workers from avian influenza (bird Flu). Department of Health and Human Services, Cincinnati
13. World Health Organization. https://www.who.int/influenza/human_animal_interface/en/. Accessed 5 Sept 2020
14. Veerman RE, Akpınar GG, Eldh M, Gabrielsson S (2019) Immune cell-derived extracellular vesicles—functions and therapeutic applications. *Trends Mol Med* 25:382–394
15. Moola N, Dang PK, Farnir F, Ton VD, Binh DV, Leroy P, Antoine-Moussiaux N (2011) The Ri chicken breed and livelihoods in North Vietnam: characterization and prospects. *J Agr Rural Dev Trop* 11:257–69
16. Seyama T, Ko J, Ohe M, Sasaoka N, Okada A, Gomi H, Yoneda A, Ueda J, Nishibori M, Okamoto S (2006) Population research of genetic polymorphism at amino acid position 631 in chicken Mx protein with differential antiviral activity. *Biochem Genet* 44:432–443
17. Berlin S, Qu L, Li X, Yang N, Ellegren H (2008) Positive diversifying selection in avian Mx genes. *Immunogenetics* 60:689
18. Sironi L, Williams JL, Moreno-Martin AM, Ramelli P, Stella A, Jianlin H, Weigend S, Lombardi G, Cordioli P, Mariani P (2008) Susceptibility of different chicken lines to H7N1 highly pathogenic avian influenza virus and the role of Mx gene polymorphism coding amino acid position 631. *Virology* 380:152–156

19. Kaufman J (1999) Co-evolving genes in MHC haplotypes: the "rule" for nonmammalian vertebrates? *Immunogenetics* 50:228–236
20. Miller MM, Bacon LD, Hala K, Hunt HD, Ewald SJ, Kaufman J, Zoorob R, Briles WE (2004) 2004 Nomenclature for the chicken major histocompatibility (B and Y) complex. *Immunogenetics* 56:261–279
21. Miller MM, Taylor RL Jr (2016) Brief review of the chicken major histocompatibility complex: the genes, their distribution on chromosome 16, and their contributions to disease resistance. *Poult Sci* 95:375–392
22. Ewald S, Ye X, Avendano S, McLeod S, Lamont S, Dekkers J (2007) Associations of BF2 alleles with antibody titres and production traits in commercial pure line broiler chickens. *Anim Genet* 38:174–176
23. Boonyanuwat K, Thummabuttra S, Sookmanee N, Vatchavalkhu V, Siripholvat V (2006) Influences of major histocompatibility complex class I haplotypes on avian influenza virus disease traits in Thai indigenous chickens. *Anim Sci* 77:285–289
24. Huprikar J, Rabinowitz S (1980) A simplified plaque assay for influenza viruses in Madin-Darby kidney (MDCK) cells. *J Virol Methods* 1:117–120
25. Hong Y, Lee J, Vu TH, Lee S, Lillehoj HS, Hong YH (2020) Immunomodulatory effects of avian β -defensin 5 in chicken macrophage cell line. *Res Vet Sci* 132:81–87
26. FastQC v0.11.7. <http://www.bioinformatics.babraham.ac.uk/projects/fastqc/>. Accessed 2 Oct 2019
27. Cutadapt 1.16. <https://cutadapt.readthedocs.org/en/stable/>. Accessed 2 Oct 2019
28. miRBase v21. <http://www.mirbase.org/>. Accessed 2 Oct 2019
29. RNAcentral 10.0. <https://rnacentral.org/>. Accessed Oct 2019
30. miRDeep2. <https://www.mdc-berlin.de/content/mirdeep2-documentation>. Accessed 2 October 2019
31. miRDB. <http://www.mirdb.org/>. Accessed 15 Nov 2019
32. gProfiler. <http://biit.cs.ut.ee/gprofiler/gost>. Accessed 20 Nov 2019
33. miRNet. <https://www.mirnet.ca/>. Accessed 8 Dec 2020
34. miRBase. <http://microrna.sanger.ac.uk/sequences/ftp.shtml>. Accessed 16 Nov 2019
35. Livak KJ, Schmittgen TD (2001) Analysis of relative gene expression data using real-time quantitative PCR and the $2^{-\Delta\Delta CT}$ method. *Methods* 25:402–408
36. Gruenberg J, Van der Goot FG (2006) Mechanisms of pathogen entry through the endosomal compartments. *Nat Rev Mol Cell Biol* 7:495–504
37. Kosaka N, Iguchi H, Hagiwara K, Yoshioka Y, Takeshita F, Ochiya T (2013) Neutral sphingomyelinase 2 (nSMase2)-dependent exosomal transfer of angiogenic microRNAs regulate cancer cell metastasis. *J Biol Chem* 288:10849–10859
38. Koumangoye RB, Sakwe AM, Goodwin JS, Patel T, Ochieng J (2011) Detachment of breast tumor cells induces rapid secretion of exosomes which subsequently mediate cellular adhesion and spreading. *PLoS One* 6:e24234
39. Koppers-Lalic D, Hackenberg M, Bijnsdorp IV, van Eijndhoven MA, Sadek P, Sie D, Zini N, Middeldorp JM, Ylstra B, de Menezes RX (2014) Nontemplated nucleotide additions distinguish the small RNA composition in cells from exosomes. *Cell Rep* 8:1649–1658
40. Frank F, Sonenberg N, Nagar B (2010) Structural basis for 5'-nucleotide base-specific recognition of guide RNA by human AGO2. *Nature* 465:818–822
41. Li Z-j, Zhang Y-p, Li Y, Zheng H-w, Zheng Y-s, Liu C-j (2014) Distinct expression pattern of miRNAs in Marek's disease virus infected-chicken splenic tumors and non-tumorous spleen tissues. *Res Vet Sci* 97:156–161
42. Peng X, Gao Q, Zhou L, Chen Z, Lu S, Huang H, Zhan C, Xiang M (2015) MicroRNAs in avian influenza virus H9N2-infected and non-infected chicken embryo fibroblasts. *Genet Mol Res* 14:9081–9091
43. Yu Z, Gao X, Liu C, Lv X, Zheng S (2017) Analysis of microRNA expression profile in specific pathogen-free chickens in response to reticuloendotheliosis virus infection. *Appl Microbiol Biotechnol* 101:2767–2777
44. Wang C, Zhou B, Liu M, Liu Y, Gao R (2017) miR-126-5p restoration promotes cell apoptosis in cervical cancer by targeting Bcl2l2. *Oncol Res* 25:463–470
45. Chen J, Wang Z, Bi D, Hou Y, Zhao Y, Sun J, Peng X (2015) gga-miR-101-3p plays a key role in *Mycoplasma gallisepticum* (HS strain) infection of chicken. *Int J Mol Sci* 16:28669–28682
46. Luo W, Lin S, Li G, Nie Q, Zhang X (2016) Integrative analyses of miRNA-mRNA interactions reveal let-7b, miR-128 and MAPK pathway involvement in muscle mass loss in sex-linked dwarf chickens. *Int J Mol Sci* 17:276
47. Ji J, Shang H, Zhang H, Li H, Ma J, Bi Y, Xie Q (2017) Temporal changes of microRNA gga-let-7b and gga-let-7i expression in chickens challenged with subgroup J avian leukosis virus. *Vet Res Commun* 41:219–226
48. Yu Y, Zhang J, Jin Y, Yang Y, Shi J, Chen F, Han S, Chu P, Lu J, Wang H (2018) MiR-20a-5p suppresses tumor proliferation by targeting autophagy-related gene 7 in neuroblastoma. *Cancer Cell Int* 18:5
49. Zhang G, Liu X, Wang W, Cai Y, Li S, Chen Q, Liao M, Zhang M, Zeng G, Zhou B (2016) Down-regulation of miR-20a-5p triggers cell apoptosis to facilitate mycobacterial clearance through targeting JNK2 in human macrophages. *Cell Cycle* 15:2527–2538
50. Sun Y, Liu W-Z, Liu T, Feng X, Yang N, Zhou H-F (2015) Signaling pathway of MAPK/ERK in cell proliferation, differentiation, migration, senescence and apoptosis. *J Recept Sig Transd* 35:600–604
51. Lee DC, Cheung C-Y, Law AH, Mok CK, Peiris M, Lau AS (2005) p38 mitogen-activated protein kinase-dependent hyperinduction of tumor necrosis factor alpha expression in response to avian influenza virus H5N1. *J Virol* 79:10147–10154
52. Pan H, Zhang Y, Luo Z, Li P, Liu L, Wang C, Wang H, Li H, Ma Y (2014) Autophagy mediates avian influenza H5N1 pseudotyped particle-induced lung inflammation through NF- κ B and p38 MAPK signaling pathways. *Am J Physiol Lung Cell Mol Physiol* 306:L183–L195
53. Hui KP, Lee SM, Cheung C-y, Ng IH, Poon LL, Guan Y, Ip NY, Lau AS, Peiris JM (2009) Induction of proinflammatory cytokines in primary human macrophages by influenza A virus (H5N1) is selectively regulated by IFN regulatory factor 3 and p38 MAPK. *J Immunol* 182:1088–1098
54. Truong AD, Hong Y, Lee J, Lee K, Lillehoj HS, Hong YH (2017) Analysis of MAPK signaling pathway genes in the intestinal mucosal layer of necrotic enteritis-afflicted two inbred chicken lines. *Korean J Poult Sci* 44:199–209
55. Xing Z, Cardona CJ, Anunciacion J, Adams S, Dao N (2010) Roles of the ERK MAPK in the regulation of proinflammatory and apoptotic responses in chicken macrophages infected with H9N2 avian influenza virus. *J Gen Virol* 91:343–351
56. Ludwig S, Planz O, Pleschka S, Wolff T (2003) Influenza-virus-induced signaling cascades: targets for antiviral therapy? *Trends Mol Med* 9:46–52
57. Elbahesh H, Cline T, Baranovich T, Govorkova EA, Schultz-Cherry S, Russell CJ (2014) Novel roles of focal adhesion kinase in cytoplasmic entry and replication of influenza A viruses. *J Virol* 88:6714–6728
58. Zhu Z, Qi Y, Ge A, Zhu Y, Xu K, Ji H, Shi Z, Cui L, Zhou M (2014) Comprehensive characterization of serum microRNA profile in response to the emerging avian influenza A (H7N9) virus infection in humans. *Viruses* 6:1525–1539
59. Wang Y, Brahmakshatriya V, Zhu H, Lupiani B, Reddy SM, Yoon B-J, Gunaratne PH, Kim JH, Chen R, Wang J (2009) Identification of differentially expressed miRNAs in chicken lung and trachea with avian influenza virus infection by a deep sequencing approach. *BMC Genomics* 10:512
60. Wang Y, Brahmakshatriya V, Lupiani B, Reddy SM, Soibam B, Benham AL, Gunaratne P, Liu H-c, Trakooljul N, Ing N (2012) Integrated analysis of microRNA expression and mRNA transcriptome in lungs of avian influenza virus infected broilers. *BMC Genomics* 13:278
61. Lam W-Y, Yeung AC-M, Ngai KL-K, Li M-S, To K-F, Tsui SK-W, Chan PK-S (2013) Effect of avian influenza A H5N1 infection on the expression of microRNA-141 in human respiratory epithelial cells. *BMC Microbiol* 13:104
62. bowtie. <http://bowtie-bio.sourceforge.net/index.shtml>. Accessed 2 Nov 2019

Publisher's Note

Springer Nature remains neutral with regard to jurisdictional claims in published maps and institutional affiliations.